Lanthanide-Dependent Regulation of Methylotrophy in *Methylobacterium aquaticum* Strain 22A

Sachiko Masuda,[a,b] Yutaka Suzuki,[c] Yoshiko Fujitani,[a] Ryoji Mitsui,[d] Tomoyuki Nakagawa,[e] Masaki Shintani,[f] Akio Tani[a]

[a]Institute of Plant Science and Resources, Okayama University, Okayama, Japan
[b]Advanced Low Carbon Technology Research and Development Program, Japan Science and Technology Agency, Tokyo, Japan
[c]Department of Computational Biology and Medical Sciences, University of Tokyo, Chiba, Japan
[d]Department of Biochemistry, Faculty of Science, Okayama University of Science, Okayama, Japan
[e]Faculty of Applied Biological Science, Gifu University, Gifu, Japan
[f]Department of Engineering, Graduate School of Integrated Science and Technology, Shizuoka University, Shizuoka, Japan

ABSTRACT *Methylobacterium* species are representative of methylotrophic bacteria. Their genomes usually encode two types of methanol dehydrogenases (MDHs): MxaF and XoxF. The former is a Ca^{2+}-dependent enzyme, and the latter was recently determined to be a lanthanide-dependent enzyme that is necessary for the expression of *mxaF*. This finding revealed the unexpected and important roles of lanthanides in bacterial methylotrophy. In this study, we performed transcriptome sequencing (RNA-seq) analysis using *M. aquaticum* strain 22A grown in the presence of different lanthanides. Expression of *mxaF* and *xoxF1* genes showed a clear inverse correlation in response to La^{3+}. We observed downregulation of formaldehyde oxidation pathways, high formaldehyde dehydrogenase activity, and low accumulation of formaldehyde in the reaction with cells grown in the presence of La^{3+}; this might be due to the direct oxidation of methanol to formate by XoxF1. Lanthanides induced the transcription of AT-rich genes, the function of most of which was unknown, and genes possibly related to cellular survival, as well as other MDH homologues. These results revealed not only the metabolic response toward altered primary methanol oxidation, but also the possible targets to be investigated further in order to better understand methylotrophy in the presence of lanthanides.

IMPORTANCE Lanthanides have been considered unimportant for biological processes. In methylotrophic bacteria, however, a methanol dehydrogenase (MDH) encoded by *xoxF* was recently found to be lanthanide dependent, while the classic-type *mxaFI* is calcium dependent. XoxF-type MDHs are more widespread in diverse bacterial genera, suggesting their importance for methylotrophy. *Methylobacterium* species, representative methylotrophic and predominating alphaproteobacteria in the phyllosphere, contain both types and regulate their expression depending on the availability of lanthanides. RNA-seq analysis showed that the regulation takes place not only for MDH genes but also the subsequent formaldehyde oxidation pathways and respiratory chain, which might be due to the direct oxidation of methanol to formate by XoxF. In addition, a considerable number of genes of unknown function, including AT-rich genes, were found to be upregulated in the presence of lanthanides. This study provides first insights into the specific reaction of methylotrophic bacteria to the presence of lanthanides, emphasizing the biological relevance of this trace metal.

KEYWORDS lanthanide, methanol dehydrogenase, methylotrophs, *xoxF*

Methylobacterium species are facultative methylotrophic alphaproteobacteria. They are ubiquitous in the natural environment, being found in soil, dust, water, air, and plants (1, 2). The metabolic pathway of methanol in *Methylobacterium* species has long been studied using *Methylobacterium extorquens* strain AM1 as a model (3). This strain, like all Gram-negative methylotrophs, oxidizes methanol to formaldehyde with pyrroloquinoline quinone (PQQ)-dependent methanol dehydrogenases (MDHs). Formaldehyde is further oxidized to formate and to CO_2. In the case of *Methylobacterium* species (and many methylotrophic alphaproteobacteria) (4), formate is converted into methylene-H_4F and fixed in the serine cycle for biosynthesis of cell constituents. *Methylobacterium* species usually contain two types of MDHs, encoded by *mxaFI* and *xoxF*. MxaFI consists of large (MxaF) and small (MxaI) subunits in a Ca^{2+}-dependent PQQ-containing MDH (5). MxaFI has been considered the main and indispensable MDH under laboratory conditions. Although the exact function of XoxF was previously a mystery (6, 7), recent findings have revealed that it is a lanthanide-dependent MDH (8–11). XoxF is the first enzyme that has been shown to require lanthanide metals for its catalytic activity (12).

The genome of strain AM1 carries two *xoxF* genes (*xoxF1* and *xoxF2*) sharing 87% amino acid sequence identity. An *xoxF1* mutant showed delayed growth on methanol (6, 7), and an *mxaF* mutant can grow in the presence of lanthanides due to intact *xoxF1* (10). *xoxF1* is induced only by light lanthanides (La^{3+}, Ce^{3+}, Pr^{3+}, and Nd^{3+}), at concentrations as low as 50 to 100 nM (13). Although an *xoxF2* mutant showed no growth defect on methanol, an *xoxF1 xoxF2* double mutant did not grow on methanol at all; these genes are required for the expression of *mxaF* (6). Suppression mutants that regained growth on methanol were obtained from the double mutant, possibly due to the loss of an unknown gene function (6). In the case of the methanotrophic *Methylomicrobium buryatense* strain 5GB1C, the causative mutation in similar suppression mutants was identified in *mxaY* encoding a response regulator. This mutation partially controls the expression of MxaB, an orphan response regulator necessary for *mxa* operon expression (14, 15). Thus, the molecular mechanism for the metal-dependent expression of MDHs remains to be studied.

xoxF is found in a wider array of bacterial genomes than *mxaF* (16). XoxF proteins can be classified into at least five groups: XoxF1 from NC10 and *Proteobacteria*; XoxF2 from NC10, LW, and *Verrucomicrobia*; XoxF3 from *Proteobacteria*; XoxF4 from *Methylophilaceae*; and XoxF5 from *Proteobacteria* (note that these names are for phylogenetic groups, not specific genes) (4). They all belong to a larger PQQ-dependent alcohol dehydrogenase family, and MxaF comprises only one branch of them. Since lanthanides are not rare in the environment (17–19), methylotrophy in the presence of lanthanides might be closer to their natural lifestyle than that under lanthanide-free laboratory conditions.

Although lanthanide-dependent MDH expression has been studied, the regulation of methylotrophy in the presence of lanthanides and the genome-wide responses to lanthanides in *Methylobacterium* species have not yet been clarified. In this study, we revealed the transcriptome of *M. aquaticum* strain 22A using transcriptome sequencing (RNA-seq) to determine the genomic responses to lanthanides. The strain was isolated from a moss, *Racomitrium japonicum* (20), and capable of promoting the growth of various plants, and its complete genome information is available (21). Phylogenetically, it is distantly related to *M. extorquens* within the genus, and members of the species have been isolated frequently from plants, including rice (22). In addition to lanthanum (La) as a light lanthanide, we also used heavier metals, holmium (Ho) and lutetium (Lu), to examine their effect on the transcriptome. The analysis revealed the lanthanide-dependent regulation of MDHs and methylotrophy systems, as well as the responses of other genes whose functions are largely unknown. They therefore represent targets for investigation in order to better understand life in the presence of lanthanides.

RESULTS

Growth characteristics of strain 22A in the presence of lanthanides. We observed the growth of strain 22A on 0.5% methanol or 0.5% succinate in the presence
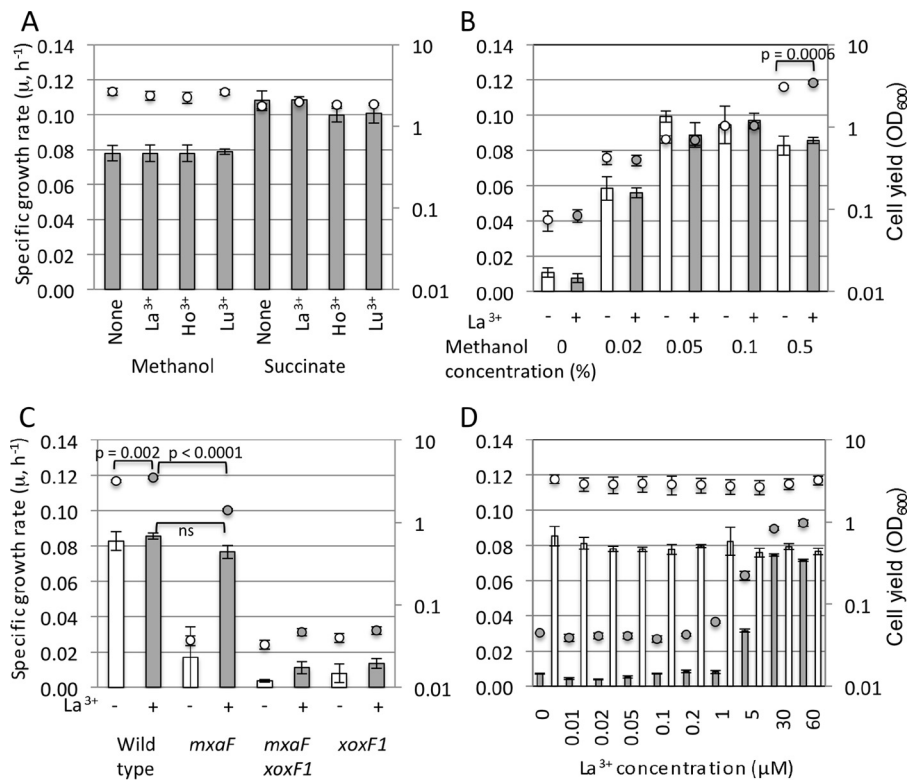
FIG 1 Growth characteristics of strain 22A and its MDH mutant derivatives. (A) Growth of strain 22A on 0.5% methanol or succinate in the presence of 30 μM La^{3+}, Ho^{3+}, and Lu^{3+}. Cell yield is shown as OD$_{600}$ values at 120 h. (B) Growth of strain 22A on methanol at different concentrations in the absence (open symbols) or presence (gray symbols) of 30 μM La^{3+}. Cell yield is shown as OD$_{600}$ values at 144 h. Statistical analysis was done using two-way analysis of variance with Bonferroni's *post hoc* test. Only a *P* value of <0.05 for the effect of La^{3+} addition is shown. (C) Growth of the strain 22A wild type and *mxaF*, *mxaF xoxF1*, and *xoxF1* mutants on 0.5% methanol in the absence (open symbols) or presence (gray symbols) of 30 μM La^{3+}. Cell yield is shown as OD$_{600}$ values at 161 h. Statistical analysis was done using two-way analysis of variance with Tukey's *post hoc* tests. Only *P* values of interest are shown. ns, not significant statistically (*P* > 0.05) between the wild type and the *mxaF* mutant in the presence of La^{3+}. (D) Growth of the strain 22A wild type (open symbols) and *mxaF* mutant (gray symbols) on 0.5% methanol in the presence of different concentrations of La^{3+}. Cell yield is shown as OD$_{600}$ values at 209 h. All experiments were performed in triplicate, and error bars show the standard deviation (SD). The specific growth rate and cell yield are shown as bars and circles, respectively.

of 30 μM lanthanides (Fig. 1A). The specific growth rate was not affected by the presence of lanthanides, irrespective of the carbon sources. As shown below, only La^{3+} among the tested lanthanides affected methylotrophy gene expression; therefore, the growth characteristics were investigated only with La^{3+}. The specific growth rate and cell yield of strain 22A were measured under limited methanol concentrations in the presence of La^{3+} (Fig. 1B). Overall, these parameters were not affected by the presence of La^{3+}. With 0.5% methanol, the cell yield was slightly higher in the presence of La^{3+}. We generated *mxaF*, *xoxF1*, and *mxaF xoxF1* deletion mutants and examined their growth on methanol. The *xoxF1* mutant and the *mxaF xoxF1* double mutant did not grow on methanol at all, whereas the *mxaF* mutant grew in the presence of La^{3+} (Fig. 1C). We isolated suppressor mutants that regained growth in the absence of lanthanides from the *xoxF* mutant (data not shown). These results indicated that *mxaF* and *xoxF1* encode Ca^{2+}-dependent and lanthanide-dependent MDH, respectively, and that *xoxF1* is necessary for *mxaF* expression, as found in strain AM1. Interestingly, the growth yield of the *mxaF* mutant in the presence of La^{3+} was significantly reduced compared to that of the wild type, but its specific growth rate was comparable to that of the wild type (Fig. 1C). The specific growth rate and cell yield of the wild type were not affected by La^{3+} at different concentrations (Fig. 1D). In contrast, those of the *mxaF*

A

B

C
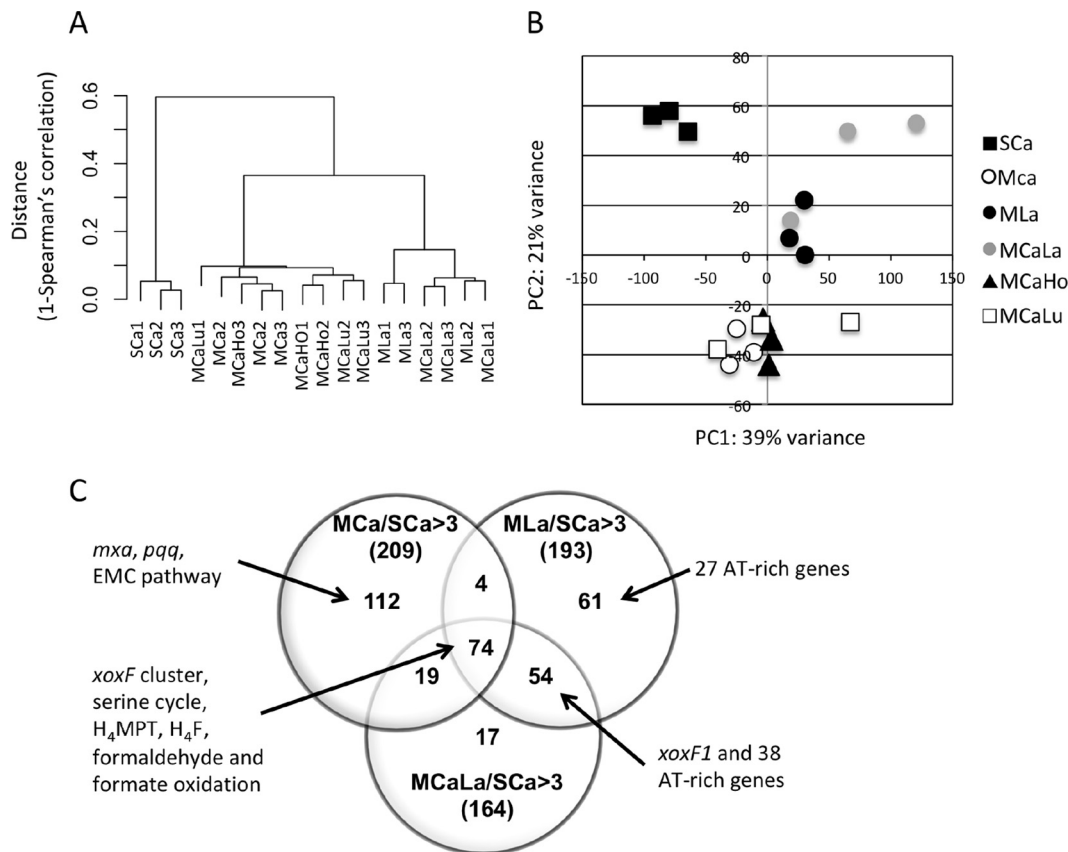
FIG 2 (A) Dendrogram based on the log$_2$-transformed expression data of all CDSs, according to Ward's clustering method as a distance measure with Spearman's 1 correlation. (B) Principal-component analysis based on the log$_2$-transformed expression data of all CDSs. (C) Venn diagram of the number of differentially expressed CDSs. Upregulated CDS numbers under the MCa, MLa, and MCaLa conditions compared to the SCa condition are counted (fold change, >3; $P < 0.05$ under any of the conditions).

mutant increased depending on the La^{3+} concentration up to 30 μM. Thus, its methylotrophic growth was completely dependent on La^{3+}. In addition, 30 μM La^{3+} was considered sufficient to achieve the full growth rate depending on XoxF1 in our experimental settings.

Overview of RNA-seq data. We isolated RNA from the cells grown under six conditions, and performed RNA-seq analysis, as detailed in Materials and Methods. As carbon sources, the cells were grown on succinate in the presence of 30 μM Ca^{2+} (SCa condition) or methanol (methanol conditions). For the methanol conditions, metal supplementations with CaCl$_2$ (MCa condition), LaCl$_3$ (MLa), CaCl$_2$ plus LaCl$_3$ (MCaLa), CaCl$_2$ plus HoCl$_3$ (MCaHo), and CaCl$_2$ plus LuCl$_3$ (MCaLu) were added. The statistics and expression data of the RNA-seq experiment are summarized in Tables S1, S2, and S3 in the supplemental material. Hierarchal clustering (Fig. 2A) and principal-component analysis (Fig. 2B) suggest that the expression profile of the SCa condition was distinct from the methanol conditions. The profiles of the MLa and MCaLa conditions were clearly different from the rest.

The fold change analysis for the MCa, MLa, and MCaLa conditions compared to the SCa condition (cutoff, >3-fold changes; $P < 0.05$ under any of the conditions) (Fig. 2C) identified 73 genes that were consistently upregulated under the methanol conditions and were thus considered to be important for methylotrophy, irrespective of the metals (Ca^{2+} or La^{3+}). They include those involved in the XoxF cluster (but not *xoxF1*), serine cycle, tetrahydromethanopterin (H$_4$MPT) pathway, tetrahydrofolate (H$_4$F) pathway, and formaldehyde and formate oxidation. The other distinguishing biological functions were ATPases, chemotaxis proteins, and those involved in flagellar synthesis (Table S3).

The upregulated genes under the MCa condition, but not under the MLa and MCaLa conditions, compared to the SCa condition, contained 112 genes involved in the *mxa* cluster, *pqq* cluster, and ethylmalonyl coenzme A (CoA) (EMC) pathway. The other distinguishing functions are ATPases, ABC transporters, and chemotaxis proteins. The genes upregulated under the MLa or MCaLa conditions, but not the MCa condition, included numerous AT-rich genes (GC content of <55%), whereas the average GC content of the strain 22A genome was 69.1%.

Expression profiles for catabolic methylotrophic pathways. The expression of the genes related to methylotrophy under the SCa, MCa, MLa, and MCaLa conditions is summarized in Fig. 3. The addition of Ho^{3+} and Lu^{3+} did not cause a significant difference in the expression profile of these genes.

The structure of the *mxa* cluster encoded in the largest plasmid is well conserved compared to that in strain AM1 (see Fig. S1A in the supplemental material). *mxaB* is missing from the cluster, but we found a homologue to AM1 MxaB called MxcE2 with 50% identity in the strain 22A chromosome, which is listed in Fig. 3. Overall, *mxa* genes were highly upregulated under the MCa condition compared to the SCa condition and clearly repressed under the MLa and MCaLa conditions compared to the MCa condition. The expression of *mxcE2* did not change under these conditions.

The *mxbDM* genes are necessary for *mxaF* expression (23), and the *mxcEQ* genes are necessary for *mxbDM* expression (24) in strain AM1. Both clusters encode sensor kinases (MxcQ and MxbD) and response regulators (MxcE and MxbM). Among these genes, only *mxbD* was upregulated under the MCa condition.

xoxF1 is clustered with *gloB*, *cytC*, *mxaJ2*, *pspE*, and *fabG* (Fig. S1B). These genes were upregulated under the methanol conditions—particularly strongly in the presence of La^{3+}. The two genes upstream of the cluster (*ansB* and c05205) did not respond to methanol. The expression profiles of *mxa* and *xox* clusters showed a striking inverse correlation depending on the presence of La^{3+}. The functions of *gloB* and *pspE* associated with *xoxF1* remain unknown and to be characterized. They often cluster with *xoxF4*- and *xoxF5*-type gene clusters (16).

PQQ is synthesized by PqqABCDEFG proteins. The expression of $pqqA_1A_2$ was more upregulated under the methanol conditions than under the SCa condition. The *pqqB-CDE* genes were upregulated only under the MCa condition. The *pqqFG* genes were not responsive to methanol and metals.

Formaldehyde may be oxidized by aldehyde dehydrogenases. We found two genes encoding aldehyde dehydrogenase upregulated under the methanol conditions (*putA* and c22865). Their substrate specificity is unknown. The absence of signal peptides (analyzed by the SignalIP 4.1 server) suggests their intracellular localization; therefore, they are not involved in the direct oxidation of formaldehyde in the periplasm. Dye-linked formaldehyde dehydrogenases were purified from three methylotrophs, and the protein from *M. capsulatus* was identified as sulfide/quinone reductase (MCA2155) or flavin adenine dinucleotide (FAD)-dependent pyridine nucleotide-disulfide oxidoreductase (16). We found three homologues (*hcaD*) with 22 to 30% identities. Their expression was, however, low under the methanol conditions, suggesting their unrelatedness to methylotrophy in strain 22A. In addition, strain 22A has the glutathione-dependent formaldehyde dehydrogenase pathway (glutathione [GSH] pathway); its genome carries *hgd* and *fgh* (see Fig. S2 in the supplemental material) but not the gene encoding glutathione-dependent formaldehyde-activating enzyme (Gfa) (25). Thus, *S*-hydroxymethyl glutathione will be spontaneously produced in strain 22A. The upregulation of these genes under the methanol conditions suggests their involvement in formaldehyde oxidation. The expression of *hgd* was lower under the MLa condition than under the MCa condition. Methylene-H_4MPT can be formed spontaneously or by the formaldehyde-activating enzyme, which is further transformed to formate via the H_4MPT pathway. Methylofuran was recently identified in strain AM1, and it carries a C_1 unit from formyl-H_4MPT in the pathway (26). The genes involved in the pathway were all upregulated under the MCa condition compared to

			Accession	Gene	Pathway/Cluster
7.6	0.1	0.1	1p33165	mxaF	
6.4	0.1	0.1	1p33170	mxaJ	
6.5	0.1	0.1	1p33175	mxaG	
8.9	0.2	0.2	1p33180	mxaI	
4.1	0.0	0.1	1p33185	mxaR	
3.8	0.1	0.1	1p33190	mxaS	
3.1	0.0	0.1	1p33195	mxaA	
4.1	0.0	0.1	1p33200	mxaK	mxa cluster
4.1	0.1	0.0	1p33205	mxaC	
3.2	0.1	0.1	1p33210	mxaL	
3.6	0.0	0.1	1p33215	mxaD	
2.9	0.1	0.1	1p33220	mxaE	
4.8	0.1	0.1	1p33225	mxaH	
2.8	0.3	0.3	1p33240	mxaW	
3.0	1.6	2.3	1p33245		
0.9	0.7	0.9	c06410	mxcE2	
3.7	0.8	1.4	c05310	mxbD	
0.8	0.8	0.7	c05305	mxbM	mxa, xox regulation
1.3	1.4	1.5	c14840	mxcQ	
1.4	1.2	1.4	c14835	mxcE	
1.2	6.8	7.5	c05210	gloB	
2.6	65	75	c05215	xoxF1	
8.4	70	100	c05220	cytC	xox cluster
4.6	37	46	c05225	mxaJ	
4.8	19	23	c05230	pspE	
0.6	1.7	1.4	c05235	fabG	
4.9	3.2	1.3	c05300	pqqA1	
3.3	2.2	1.0	c05295	pqqA2	
4.1	0.8	0.9	c05290	pqqB	
3.0	0.9	1.1	c05285	pqqC	pqq cluster
3.8	0.7	1.4	c05280	pqqD	
2.2	0.8	0.9	c05275	pqqE	
0.7	0.7	0.8	c10575	pqqF	
0.6	0.6	0.7	c10580	pqqG	
7.1	13	10	c22860	putA	
3.8	3.4	4.6	c22865		
0.7	0.5	0.7	c24660	coxL	
0.7	0.7	0.8	c10895	putA	
0.8	0.6	0.6	c24650	hcaD	Aldehyde oxidation
0.5	0.3	0.5	1p36810	hcaD	
0.5	1.1	0.8	c07385	hcaD	
9.4	3.8	5.1	c21490	hgd	
5.9	3.9	3.9	c21495	fah	
12	6.2	9.1	c16490	fae	
8.6	4.2	5.4	1p31155	fae	
4.6	2.4	2.9	c16460	mtdB	
6.3	3.1	3.7	c16475	mch	
4.5	1.9	2.1	c16480	rimK	H4MPT pathway
11	2.1	2.8	c16485	orf7	
4.2	2.0	2.2	c16435	fhcC	
3.9	1.8	1.9	c16440	fhcD	
4.7	2.1	2.5	c16445	fhcA	
4.8	2.2	2.4	c16450	fhcB	
13	4.1	4.4	c23990		
1.1	0.6	0.7	1p32780	lysR	
28	20	23	1p32795	fdh2A	
36	30	30	1p32790	fdh2B	
48	22	30	1p32785	fdh2C	
18	6.4	11	1p32805	fdh2D	Formate oxidation
19	19	15	1p32800	fdhD	
1.7	1.3	1.3	c07835	fdh3A	
1.5	1.5	1.3	c07830	fdh3B	
1.8	1.4	1.4	c07825	fdh3C	
4.3	3.2	2.7	c07840		
0.2	0.6	0.4	1p38175	fdh4A	
24	21	30	c20030	ftfL	
27	32	40	c19270	fch	H4F pathway
28	32	36	c19275	mtdA	
7.1	9.7	12	c24915	glyA	
228	186	251	c19285	sga	
20	15	26	c19280	hprA	
6.7	2.2	3.5	c06910	gck	
1.2	1.4	1.3	c17025	eno	
83	100	110	c19255	ppc	Serine cycle
1.5	1.1	1.5	c00515	ppc2	
0.4	0.7	0.8	c03115	pckA	
0.4	0.6	0.6	c11320	mdh	
126	122	169	c19265	mtkA	
128	163	149	c19260	mtkB	
98	149	149	c19250	mcl	
0.8	0.8	1.0	1p37465	phaA	
1.5	1.4	1.5	1p37470	phaB	
32	6.1	12	c17200	croR	
4.1	2.7	3.4	1p32000	ccrA	
3.4	1.9	2.0	c02915	gloA	
2.3	1.4	1.8	1p32005	meaA	Ethylmalonyl-CoA pathway
2.8	1.9	2.2	c07055	ibd2	
0.9	0.8	1.0	c24130	meaC	
1.9	1.0	1.2	c18385	citE	
2.4	1.5	1.6	c15525	pccA	
3.4	2.0	2.4	1p33770	pccB	
2.2	1.3	1.4	c24700	mcmA	
2.5	2.0	1.9	c08405	mcmB	

			Accession	Gene	Pathway/Cluster
1.4	0.8	0.9	c06395	phaC	
12	4.7	6.8	c02990	depA	
0.6	0.8	0.8	c27430	depA	PHB cycle
0.7	0.8	1.0	c24375	fabG	
1.3	0.5	0.8	c17100	atoD	
0.9	0.9	1.0	c17105	atoA	
0.4	0.5	0.6	c11315	sucC	
0.4	0.5	0.5	c11310	sucD	
0.4	0.3	0.4	c24165	sdhA	
0.5	0.4	0.5	c24180	sdhB	
0.5	0.2	0.3	c24155	sdhC	
0.4	0.2	0.3	c24160	sdhD	
0.9	0.8	1.0	1p37295	fumC	TCA cycle
2.9	2.3	2.9	2p40740	fumC	
0.3	0.3	0.3	c12695	ttdA	
0.4	0.5	0.6	c13015	gltA	
1.1	1.2	1.4	c15955	acnA	
0.9	1.4	1.4	c12150	icd	
0.4	0.5	0.6	c11305	sucA	
0.8	0.9	1.0	c02835	nuoA	
1.0	0.9	1.2	c02840	nuoB	
1.0	0.8	1.2	c02845	nuoC	
0.9	1.0	1.0	c02850	nuoD	
0.8	0.9	1.1	c02855	nuoE	
0.6	0.7	0.8	c02860	nuoF	
0.7	0.7	0.7	c02865	nuoG	NADH-quinone oxidoreductase (Ndh-1)
0.6	0.8	0.8	c02870	nuoH	
0.6	1.1	0.9	c02875	nuoI	
0.7	0.8	0.8	c02880	nuoJ	
0.8	1.3	1.1	c02885	nuoK	
1.0	1.0	1.2	c02890	nuoL	
0.8	1.2	1.1	c02895	nuoM	
0.8	0.8	0.9	c02900	nuoN	
0.5	0.5	0.5	1p35725	nuoN	
0.6	0.4	0.4	1p35735	nuoM	
0.5	0.4	0.4	1p35740	nuoL	
0.4	0.3	0.4	1p35745	nuoK	NADH-quinone dehydrogenase (Ndh-1)
0.7	0.4	0.4	1p35750	nuoJ	
0.4	0.2	0.3	1p35760	nuoH	
0.2	0.2	0.2	1p35765	nuoA	
2.5	0.8	1.2	1p31735	ndh	NADH-quinone dehydrogenase (Ndh-2)
1.4	0.9	1.3	1p33330	qcrA	
0.9	1.0	1.2	1p33335	qcrB	Ubiquinol-cytochrome c reductase
1.1	0.8	1.2	1p33340	cyt1	
0.4	0.4	0.5	1p36825	cydA	
0.4	0.4	0.4	1p36830	appB	Cytochrome bd oxidase
1.2	0.6	0.7	5p70115	appB	
1.6	1.5	1.6	1p32770	cyoB	
1.8	1.3	1.8	1p32775	cyoA	
1.6	1.6	1.7	1p32750	cyoC	Cytochrome c oxidase complex (Cox1)
1.2	1.3	1.2	1p32755	cox11	
1.9	1.1	1.5	1p32765	cyoE	
0.7	0.8	0.9	c08345	cyoB	
0.8	0.8	1.0	c08340	cyoA	Cytochrome c oxidase complex (Cox2)
0.7	0.7	1.0	c08350	cyoC	
0.9	0.6	0.7	1p34895	cyoB	
0.7	0.6	0.7	1p34890	cyoA	Cytochrome c oxidase complex (Cox3)
0.9	0.7	0.7	c26125	ctaA	
0.3	0.4	0.4	c08985	cyoB	
0.3	0.3	0.4	c08990	cyoA	Cytochrome o ubiquinol oxidase complex (Cyo)
0.2	0.5	0.4	c08980	cyoC	
0.2	0.5	0.5	c08975	cyoD	
0.7	0.4	0.7	1p31455	ccoN	
0.6	0.3	0.4	1p31460	ccoO	
0.5	0.4	0.6	1p31470	cccA	Cytochrome c oxidase cbb3-type
0.6	0.4	1.2	1p31465		
0.7	0.8	1.1	1p35110	ccoN	
0.7	0.5	0.6	1p35105	ccoO	
0.4	0.6	0.6	1p35095	cccA	Cytochrome c oxidase cbb3-type
0.8	0.6	1.4	1p35100		
1.5	2.0	2.1	1p30825	atpB	
1.1	1.2	1.3	1p30810		
1.5	1.4	2.0	1p30815	atpF	
1.9	3.3	2.7	1p30820	atpE	
1.4	1.5	1.5	c11710	atpA	F-type H+-transporting ATPase
1.2	1.6	1.4	c11700	atpD	
1.4	1.3	1.4	c11705	atpG	
1.2	0.9	1.0	c11715	atpH	
1.0	1.0	1.1	c11695	atpC	

SCa MCa MLa MCaLa

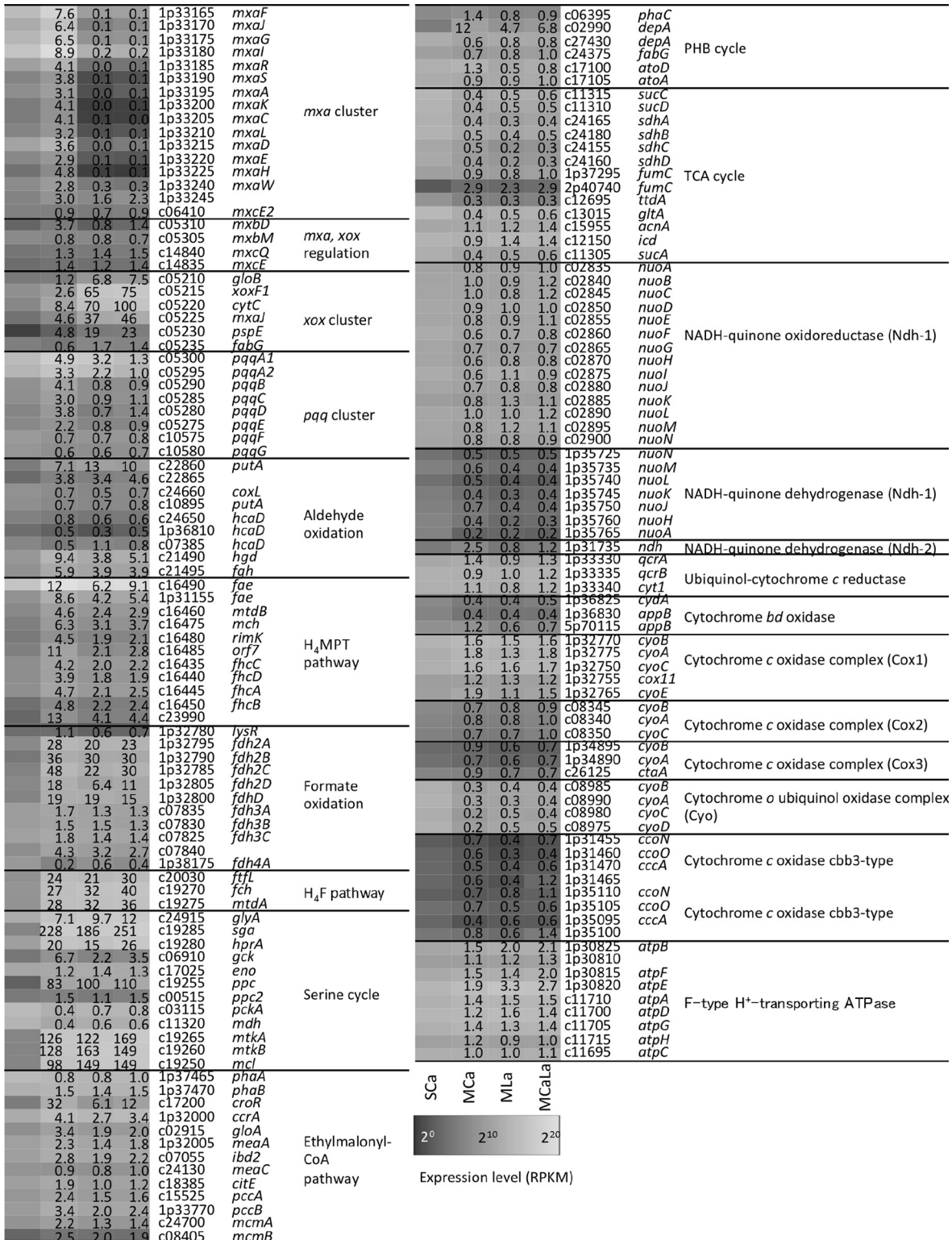2^0 2^{10} 2^{20}

Expression level (RPKM)

FIG 3 Heat map of the gene expression involved in methylotrophy and related pathways under the SCa, MCa, MLa, and MCaLa conditions. Gene accession numbers are shown without the suffix (Maq22A_). Fold change values against the SCa condition are shown in the heat map.

the SCa condition, but were relatively repressed in the presence of La^{3+} compared to the MCa condition.

We annotated the molybdenum-dependent formate dehydrogenase complex (fdh2ABCD), cytochrome-linked formate dehydrogenase complex (fdh3ABC and

c07840), and *fdh4A* for formate oxidation. Fdh2 complex was upregulated under the methanol conditions, and the expression of Fdh2C and 2D components was slightly lower under the MLa condition than under the MCa condition. The expression of *fdh4A* was high under the SCa condition and lowest under the MCa condition, the meaning of which is unknown.

The H_4F pathway converts formate to methylene H_4F, which is further used as C_1 supply for the serine cycle. The pathway was upregulated under the methanol conditions; however, expression of the corresponding genes was not responsive to the presence of La^{3+}.

Expression profiles for anabolic methylotrophic pathways. All genes for the serine cycle (see Fig. S3 in the supplemental material) were upregulated under the methanol conditions, except for *eno* and *ppc2* (Fig. 3). Two molecules of acetyl-CoA produced in the serine cycle are converted to methylmalonyl-CoA through the EMC pathway to supply glyoxylate for the serine cycle (27, 28). Most of the genes in the pathway were upregulated under the methanol conditions, except for *phaA*, *phaB*, and *meaC*. The genes for the EMC pathway were slightly downregulated under the MLa condition compared to the MCa condition. Within the poly-β-hydroxybutyrate (PHB) cycle, *depA* (c02990) was induced higher under the methanol conditions than under the SCa condition. Expression of *depA* (c02990) and *atoD* was higher under the MCa condition than under the MLa condition. The genes for the tricarboxylic acid (TCA) cycle were highly expressed under the SCa condition, which was expected when succinate was the carbon source. Their expression was not responsive to the presence of La^{3+}, except for *sdhC* (c24155).

The expression of one of the NADH dehydrogenase (Ndh-1) clusters encoded in the plasmid pMaq22A-1 (1p35725-1p35765) was relatively low compared to that of the other and was lower under the methanol conditions. The expression of another NADH-quinone dehydrogenase (Ndh-2) was high only under the MCa condition. Ndh-2 does not pump protons, but is important for higher metabolic flux and increased carbon flux into biosynthetic pathways (29, 30). The meaning of this upregulation is currently unclear. Among seven different types of cytochrome oxidases, the expression of components in cytochrome *o*-type ubiquinol oxidase was lower under the methanol conditions than under the SCa condition, and expression was even lower under the MCa condition than under the MLa condition. The expression of F-type ATPase genes was higher under the methanol conditions than under the SCa condition, and some components (*atpB*, *atpE*, and *atpD*) showed slightly higher expression under the MLa and MCaLa conditions than under the MCa condition.

Lanthanide-dependent expression of MDH-like genes. We found four more MDH-like genes besides *mxaF* and *xoxF1* in the strain 22A genome. One of them is named *xoxF2*, the deduced amino acid sequence of whose product has 71% identity to XoxF1 (Fig. 4A). The other three proteins showed 30 to 35% identity to MxaF, XoxF1, and XoxF2. The important amino acid residue (Asp301 in *Methylacidiphilum fumariori-cum* SolV XoxF1), which is typical and diagnostic of XoxF-type MDHs and considered necessary for lanthanide ion binding (11), is conserved in four of them.

As already shown in Fig. 3, the expression of *mxaF* and *xoxF1* was clearly switched by the presence of La^{3+} (Fig. 4B), suggesting that strain 22A uses XoxF1 preferentially when La^{3+} is available and uses MxaF only when La^{3+} is absent. The expression of the other four genes was relatively low under these conditions. XoxF2 and 1p32165 showed no clear expression patterns. *xoxF2* might be a pseudogene, because its open reading frame (ORF) seemed to be truncated and does not contain a signal peptide. The expression of c07235 was induced, and 1p30675 was repressed, in the presence of La^{3+}. These responses correlate with the presence of amino acids that bind lanthanides: e.g., XoxF1 and c07235 have an Asp residue at position 301 that binds lanthanides, while MxaF and 1p30675 have Ala at position 301 that interacts with calcium.

Upregulated genes in the presence of lanthanides. We noticed that AT-rich genes showed high relative expression in the presence of lanthanides compared to the
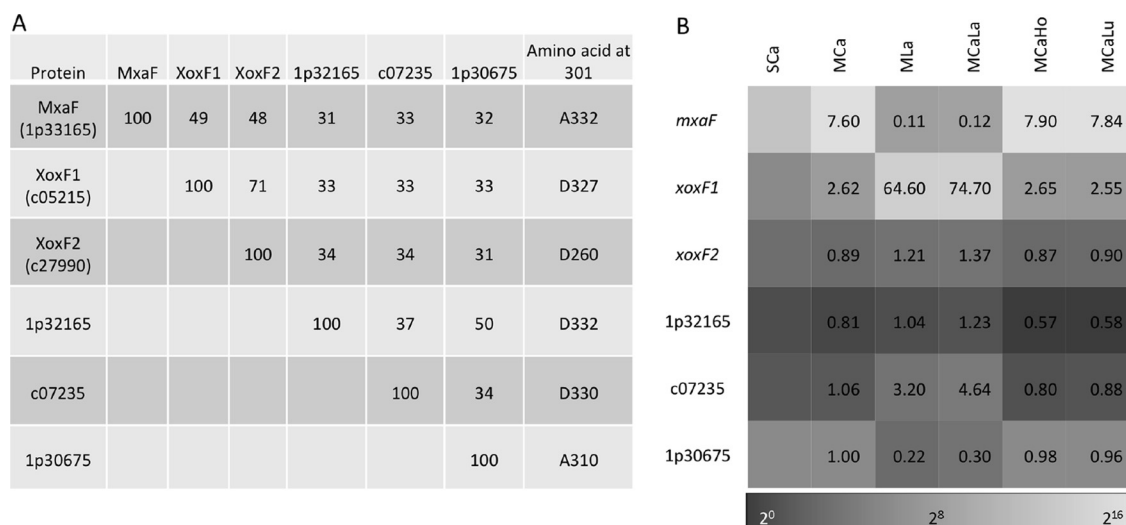
A

Protein	MxaF	XoxF1	XoxF2	1p32165	c07235	1p30675	Amino acid at 301
MxaF (1p33165)	100	49	48	31	33	32	A332
XoxF1 (c05215)		100	71	33	33	33	D327
XoxF2 (c27990)			100	34	34	31	D260
1p32165				100	37	50	D332
c07235					100	34	D330
1p30675						100	A310

B

	SCa	MCa	MLa	MCaLa	MCaHo	MCaLu
mxaF		7.60	0.11	0.12	7.90	7.84
xoxF1		2.62	64.60	74.70	2.65	2.55
xoxF2		0.89	1.21	1.37	0.87	0.90
1p32165		0.81	1.04	1.23	0.57	0.58
c07235		1.06	3.20	4.64	0.80	0.88
1p30675		1.00	0.22	0.30	0.98	0.96

2^0 2^8 2^{16}

FIG 4 Properties and expression of MDH-like genes found in the strain 22A genome. (A) Pairwise identities of amino acid sequences of MDH-like genes and amino acids corresponding to position 301 (D-) in XoxF from *M. fumarioricum* SolV. (B) Heat map of MDH-like gene expression. Gene accession numbers are shown without the suffix (Maq22A_). Fold change values against the SCa condition are shown in the heat map.

MCa condition. Figure 5A and B show the expression of 89 genes with the lowest GC content (<55%) in the strain 22A genome. These genes are scattered in the genome, as shown by their locus tags. The expression of the genes with lower GC content was more impacted by lanthanides, especially under the MLa condition (Fig. 5C). It is known that AT-rich genes are silenced by nucleoid-associated proteins (NAPs) (31, 32). We found 18 NAP genes in the strain 22A genome, and their expression is summarized in Fig. S4 in the supplemental material. None of these genes showed specifically lower expression in the presence of lanthanides compared to the MCa condition, however, suggesting that NAPs may not be involved in the derepression of AT-rich genes.

In addition to AT-rich genes, we sought La^{3+}-induced genes with the following restrictions: MLa versus MCa, >2.5-fold change; MCaLa versus MCa, >2.5-fold change; MLa versus SCa, >2-fold change; GC content, >60%; genes not tRNA genes. These restrictions extracted 27 genes. They included the aforementioned five genes in the *xoxF* cluster and the quinoprotein alcohol dehydrogenase gene (c07235). The expression of the rest, 16 of which encode hypothetical proteins, is summarized in Fig. 6. The functions of these genes for methylotrophy are currently unknown and remain to be characterized; we describe their general functions in the Discussion section.

Methanol and formaldehyde oxidation activity in strain 22A. As shown above, La^{3+} had a particular impact on the expression of MDH genes and formaldehyde oxidation genes. These results prompted us to investigate the difference in the methanol and formaldehyde oxidation activities of cells grown in the presence and absence of La^{3+}. The MDH activity in the methanol-grown cells in the presence of La^{3+} was 49 mU·mg^{-1} protein, whereas that in the absence of La^{3+} was 3 mU·mg^{-1} protein (Fig. 7A). The activity toward formaldehyde was also higher in the former (95 mU·mg^{-1} protein compared to 4 mU·mg^{-1} protein). The cells grown on succinate in the presence of La^{3+} showed low activity.

Next, we quantified the formaldehyde accumulation and degradation with resting cells. The formaldehyde accumulation was faster in the cells grown in the presence of Ca^{2+} than in those grown in the presence of La^{3+}; the rates were 0.727 and 0.255 pmol formaldehyde·min^{-1}·per 10^5 cells, respectively (Fig. 7B, panel a). The formaldehyde degradation rates were comparable between them; the rates were 7.58 and 7.24 pmol formaldehyde·min^{-1}·per 10^5 cells for cells grown in the presence of Ca^{2+} and La^{3+}, respectively (Fig. 7B, panel b).

A

SCa	MCa	MLa	MCaLa	MCaHo	MCaLu	Accession	GC
1.9	9.0	3.9	3.8		7.0	c04185	(44.9)
0.9	1.4	1.0	0.9		1.2	2p42070	(53.4)
1.5	3.9	3.1	2.2		3.9	c25690	(42.5)
2.5	4.8	3.5	2.9		4.7	c12325	(45.0)
1.7	5.7	2.8	3.1		6.6	c12320	(41.8)
4.5	12	6.7	7.9		15	2p42795	(42.3)
1.8	4.3	2.2	2.7		6.3	c11175	(46.5)
0.7	6.4	2.3	1.5		5.1	c22190	(46.1)
1.9	2.9	1.7	2.6		4.9	c11180	(49.8)
1.2	3.9	2.1	2.4		4.6	2p40865	(49.2)
0.9	2.0	1.6	1.3		1.9	c06340	(51.4)
1.7	5.0	2.7	2.5		4.3	2p40895	(51.4)
2.3	9.2	4.8	4.6		9.8	c14170	(39.2)
1.1	2.7	2.2	1.5		1.9	2p40890	(50.0)
2.5	4.9	3.3	1.9		3.5	c22185	(53.8)
0.9	12	4.3	1.6		3.2	c24675	(34.9)
1.5	4.9	2.9	2.7		4.0	c05545	(43.8)
0.7	2.7	1.7	1.3		2.6	c14165	(47.0)
1.5	3.8	2.5	2.1		3.3	c06700	(51.5)
2.6	4.8	4.5	3.7		7.0	c04100	(46.5)
1.3	5.2	2.4	1.9		3.4	2p42465	(46.5)
1.5	2.3	1.7	2.2		3.9	c12810	(48.9)
1.8	12	4.5	3.5		8.3	1p36995	(43.8)
1.7	8.9	4.8	3.0		5.9	c02320	(39.2)
0.3	0.8	0.7	0.5		0.7	2p41930	(38.9)
1.7	8.8	3.0	3.4		7.9	c11595	(47.6)
2.6	5.8	3.5	3.8		8.5	c04895	(44.8)
1.0	13	3.2	2.3		7.6	1p37745	(31.8)
2.4	5.2	3.2	2.8		4.9	c19230	(48.0)
0.9	2.0	1.6	1.1		1.6	c00265	(50.0)
0.8	2.9	1.5	1.3		2.2	4p60195	(54.2)
0.9	5.1	2.2	1.6		3.6	1p37750	(45.5)
1.4	2.1	1.5	1.2		2.2	1p36990	(54.5)
1.3	14	4.7	3.2		8.2	c22160	(36.4)
2.4	15	8.3	4.8		7.3	c05175	(40.3)
0.7	2.9	1.9	1.2		1.9	c09760	(49.1)
0.8	3.7	1.6	1.5		2.3	c04150	(40.4)
2.2	6.6	4.5	4.2		6.9	c04105	(42.4)
1.2	4.9	2.7	2.1		4.3	c03305	(43.7)
1.5	1.8	1.8	1.2		1.6	c13305	(51.3)
0.6	2.3	1.4	0.7		1.2	c23010	(54.4)
1.2	16	5.3	3.1		7.5	1p37760	(31.9)
2.1	13	5.1	5.1		11	c02355	(40.0)
1.9	6.2	3.1	2.7		4.6	c18075	(52.9)
1.2	3.4	2.2	1.7		3.8	c13315	(45.5)
1.8	6.1	3.6	2.9		5.5	c22515	(42.0)
1.5	1.8	2.4	1.7		1.9	c22525	(54.8)
2.2	5.4	3.8	2.6		3.3	c27960	(54.1)
1.0	11	3.4	1.9		4.8	c23165	(39.6)
1.4	7.1	3.8	2.2		4.6	c24825	(41.7)
1.2	5.4	2.8	1.6		3.6	2p42220	(49.8)
0.8	4.8	1.9	1.0		2.4	c23160	(47.9)
1.1	5.3	2.4	2.0		3.9	c00285	(47.5)
3.9	10	5.4	6.4		13	c17665	(40.1)
3.1	19	6.7	6.3		14	c08715	(35.5)
1.5	3.9	2.2	2.5		3.5	c10940	(49.0)
1.8	4.4	2.3	1.9		2.9	2p42610	(54.8)
0.5	4.6	1.5	1.2		1.6	c12980	(48.7)
1.4	12	4.4	2.9		7.3	1p36645	(43.7)
2.3	6.7	3.8	4.1		8.5	c18425	(42.2)
1.3	3.6	2.6	2.6		5.4	1p36650	(40.1)
0.8	1.4	1.5	1.0		1.0	c25900	(46.8)

B

SCa	MCa	MLa	MCaLa	MCaHo	MCaLu	Accession	GC	Annotation
1.5	9.4	2.9	4.3		11	2p42385	(41.0)	Flp pilus assembly protein TadG
3.2	15	8.1	5.8		15	c04065	(36.7)	RelA/SpoT domain protein
0.8	6.7	2.8	1.9		4.7	c22195	(40.6)	uncharacterized conserved protein
1.2	3.7	2.0	1.8		3.5	c11600	(46.7)	ATPases
1.6	3.1	2.4	2.1		3.4	2p40465	(54.5)	ABC transporter permease
7.7	210	61	14		36	1p34445	(38.1)	SAM-dependent methyltransferases
1.7	8.3	3.9	3.0		5.9	1p38560	(37.5)	uncharacterized protein conserved in bacteria
0.8	3.3	1.8	1.6		3.0	c19760	(44.7)	putative restriction endonuclease or methylase
1.6	5.7	2.8	3.0		6.3	c05535	(45.6)	response regulator containing CheY-like receiver
0.6	2.6	1.3	0.8		1.1	c23015	(51.7)	uncharacterized phage-associated protein
2.8	8.3	4.2	4.5		8.3	c12815	(50.5)	predicted phosphoribosyltransferases
1.9	7.4	3.6	3.5		7.3	c05530	(46.5)	signal transduction histidine kinase
1.0	1.3	0.9	0.9		1.3	c27720	(50.2)	uncharacterized protein conserved in bacteria
2.0	19	7.7	4.0		10	2p42095	(37.3)	glycosyltransferase
2.2	8.4	4.1	3.6		8.6	c05525	(45.4)	ATPase components of ABC transporters with duplicated ATPase domains
3.0	10	3.7	3.5		7.7	c13280	(45.2)	adenylate cyclase, family 3
1.8	8.1	4.9	3.1		5.1	c28555	(48.6)	capsular polysaccharide biosynthesis protein
1.3	9.5	3.3	2.9		6.1	2p42080	(37.3)	Flp pilus assembly protein TadD, contains TPR repeats
1.8	13	4.4	3.2		7.8	c05690	(38.9)	conserved hypothetical protein
2.9	8.3	4.5	3.3		6.3	1p36965	(48.0)	adenylate cyclase, family 3
1.0	9.5	3.7	2.4		6.8	c28780	(41.4)	arylsulfatase regulator
4.1	16	7.5	6.9		17	c10935	(39.9)	deoxycytidine deaminase
0.9	3.8	2.0	1.3		2.2	c24550	(52.7)	ABC-type polysaccharide/polyol phosphate export systems, permease component
1.4	3.2	2.5	2.0		3.1	c20325	(49.3)	cephalosporin hydroxylase
1.2	7.6	2.9	2.3		5.1	c00275	(45.1)	predicted glycosyltransferases
1.6	14	5.2	3.7		9.8	2p42140	(38.9)	glycosyltransferase
1.0	2.2	1.7	1.1		1.4	c01855	(54.2)	50S ribosomal protein L33

Expression level (RPKM): 2^0 — 2^7 — 2^{14}

C — Fold change (against MCa condition) vs GC content of genes (%): ● MLa/MCa ● MCaLa/MCa ▲ MCaHo/MCa □ MCaLu/MCa

FIG 5 Expression response of AT-rich genes to lanthanides. (A and B) Heat maps of the expression level of the genes with low GC content (<55%) under all conditions. (A) Genes annotated as hypothetical proteins. (B) Annotated genes. The GC content of the gene is shown in parentheses. The genes are sorted to their expression level under the SCa condition. Gene accession numbers are shown without the suffix (Maq22A_). Fold change values against the SCa condition are shown in the heat map. (C) Relationship between gene GC content and fold change in expression against the MCa condition.

PQQ production and biofilm formation. The relatively low expression of the *pqq* cluster in the presence of La³⁺ (Fig. 3) prompted us to measure PQQ production by strain 22A. As shown in Fig. S5 in the supplemental material, the PQQ concentration in the spent medium was lower in the presence of La³⁺ in strain 22A grown on methanol. Thus, the decreased PQQ production was in line with the lower expression of the *pqq* cluster in the presence of La³⁺; however, its biological meaning is currently unknown since MxaF and XoxF are both PQQ-dependent MDHs.

Related to the upregulation of the diguanylate cyclase gene (Fig. 6), we monitored the colony morphology, motility, and biofilm formation of strain 22A. There was no clear morphological difference in the colonies, no difference in the motility (swimming motility under a microscope, data not shown) of the cells, and no difference in the biofilm formation in the cultures of strain 22A grown on methanol with 30 μM La³⁺ (see Fig. S6 in the supplemental material).

DISCUSSION

In this study, we used *M. aquaticum* strain 22A as a model to determine the transcriptomic profile in response to methanol and lanthanides. Strain 22A has some characteristics that differ from strain AM1 in methylotrophy. The strain 22A genome encodes glutathione-dependent formaldehyde dehydrogenase, and the strain does not
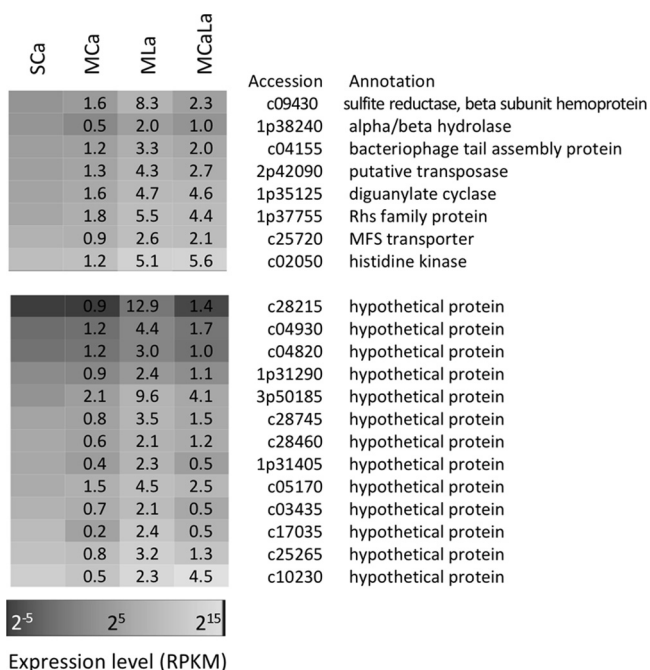
SCa	MCa	MLa	MCaLa	Accession	Annotation
	1.6	8.3	2.3	c09430	sulfite reductase, beta subunit hemoprotein
	0.5	2.0	1.0	1p38240	alpha/beta hydrolase
	1.2	3.3	2.0	c04155	bacteriophage tail assembly protein
	1.3	4.3	2.7	2p42090	putative transposase
	1.6	4.7	4.6	1p35125	diguanylate cyclase
	1.8	5.5	4.4	1p37755	Rhs family protein
	0.9	2.6	2.1	c25720	MFS transporter
	1.2	5.1	5.6	c02050	histidine kinase
	0.9	12.9	1.4	c28215	hypothetical protein
	1.2	4.4	1.7	c04930	hypothetical protein
	1.2	3.0	1.0	c04820	hypothetical protein
	0.9	2.4	1.1	1p31290	hypothetical protein
	2.1	9.6	4.1	3p50185	hypothetical protein
	0.8	3.5	1.5	c28745	hypothetical protein
	0.6	2.1	1.2	c28460	hypothetical protein
	0.4	2.3	0.5	1p31405	hypothetical protein
	1.5	4.5	2.5	c05170	hypothetical protein
	0.7	2.1	0.5	c03435	hypothetical protein
	0.2	2.4	0.5	c17035	hypothetical protein
	0.8	3.2	1.3	c25265	hypothetical protein
	0.5	2.3	4.5	c10230	hypothetical protein

2^{-5} 2^{5} 2^{15}

Expression level (RPKM)

FIG 6 Heat map of expression level of the genes extracted under restrictions of MLa versus MCa >2.5-fold change, MCaLa versus MCa >2.5-fold change, MLa versus SCa >2-fold change, GC content of >60%, and genes not tRNA genes. The genes are sorted to their expression level under the SCa condition. Fold change values against SCa condition are shown in the heat map.

grow on methylamine due to the absence of methylamine dehydrogenase. In addition, strain 22A grows on glucose but strain AM1 does not. Despite these differences, the MDH systems of MxaF and XoxF1 (and other MDH-like genes as well) are commonly found in *Methylobacterium* genomes, and almost all of the components of the metabolic pathways are shared in common.

Ho^{3+} and Lu^{3+} did not impact the growth rate of strain 22A and the expression of methylotrophy genes compared to the MCa condition (Fig. 1A; Table S3). Since *xoxF1* in strain AM1 is induced only by light lanthanides (13), these heavier lanthanides may not be recognized by strain 22A and its XoxF1 protein as well, probably due to their different ion radii. The strain 22A *mxaF* mutant showed comparable specific growth rates due to intact *xoxF1* in the presence of La^{3+}, but its growth yield was significantly lower than that of the wild type (Fig. 1C). This is discussed below with the expression data and enzyme activities. The strain 22A mutants of *xoxF1* and *xoxF1 mxaF* could not grow on methanol at all (Fig. 1C), and *xoxF2* might be a pseudogene. Thus, the necessity of *xoxF1* for *mxaF* expression seemed to also occur in strain 22A as in strain AM1, and only *mxaF* and *xoxF1* are able to support growth on methanol in strain 22A, whereas a strain AM1 *mxaF xoxF1 xoxF2* triple mutant can still grow on methanol in the presence of La^{3+} (13, 33). The strain 22A *mxaF* mutant required more than 30 µM La^{3+} to achieve its full growth rate (Fig. 1D), whereas 1 µM La^{3+} was enough for an AM1 *mxaF* mutant (33). These are the distinct differences in mutant phenotypes in strains 22A and AM1.

La^{3+} had a significant impact on the expression of methylotrophy genes in strain 22A. The most striking contrast in gene expression was observed for the switching of the *mxa* and *xox* clusters (Fig. 3). Specifically, *mxaF* and *xoxF1* showed approximately 71-fold and 24-fold induction, depending on the presence or absence of La^{3+}, respectively (Fig. 4). As suggested in strain AM1 (6, 13), *mxbD*, which has higher expression under the MCa condition than under the MLa condition in strain 22A, is considered to regulate the switching. The ligand for MxbD is currently unknown. The expression of *mxcE2* did not change under these conditions, although the *mxaB* homologue in
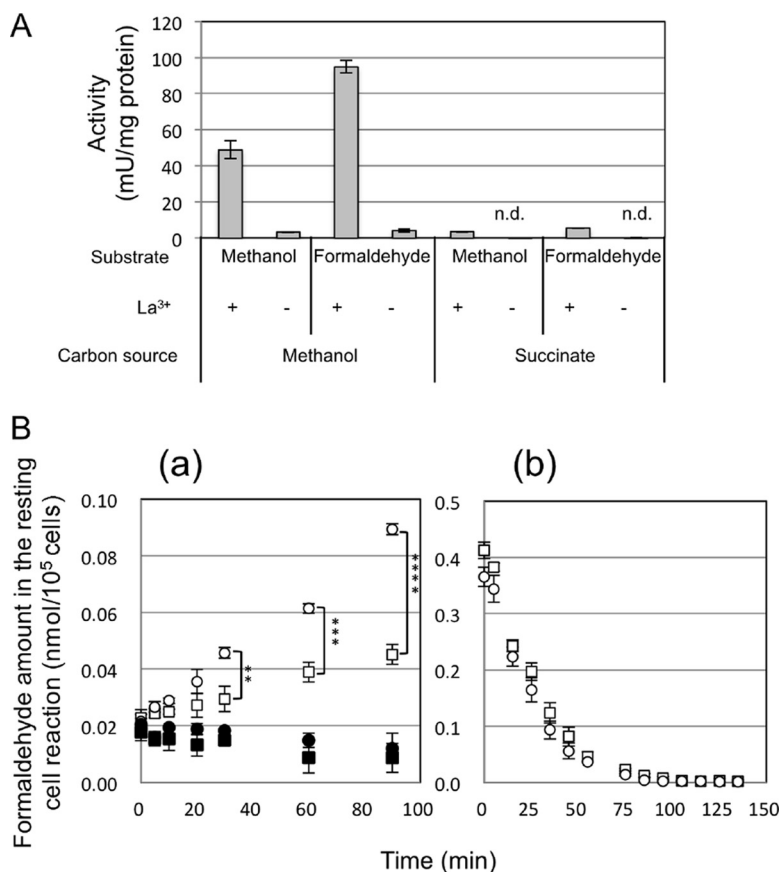
FIG 7 (A) Dehydrogenase activities toward methanol and formaldehyde in the cell-free extracts of strain 22A grown on methanol or succinate, in the presence of 30 μM CaCl$_2$, and in the absence and presence of LaCl$_3$. Activities were determined from three biological and three technical replicates. n.d., not detected. Error bars show the standard error of the mean ($n = 3$). (B) Formaldehyde production and degradation by resting cells of strain 22A pregrown on methanol in the absence and presence of La^{3+}. Production (a) and degradation (b) of formaldehyde by strain 22A cells were measured. Strain 22A was pregrown on methanol in the absence (circles) and presence (squares) of LaCl$_3$. Autoclave-killed cells were used as controls (closed symbols). The molar amounts of formaldehyde in the 200-μl reaction mixture in 96-well plates were normalized by total cell numbers (10^5 cells). Asterisks indicate statistical significance: **, $P < 0.01$; ***, $P < 0.001$; and ****, $P < 0.0001$ (Sidak's multiple-comparison test).

Methylomicrobium buryatense strain 5GB1C was reported to be lanthanide responsive and partially involved in MDH switching (14).

In addition to the MDH systems, the formaldehyde oxidation systems of GSH and H$_4$MPT pathways were downregulated in the presence of La^{3+} compared to the MCa condition. This might be explained by the direct oxidation of formaldehyde by XoxF (11, 16). The high activity toward formaldehyde (Fig. 7A) and the reduced formaldehyde production in cells grown in the presence of La^{3+} (Fig. 7B) support this explanation. When XoxF oxidized formaldehyde in the presence of La^{3+}, it would produce more reduced cytochrome *c* than MxaF produces under the MCa condition. The decreased formaldehyde generation by MDHs may lead to decreased induction of the H$_4$MPT and GSH pathways, which further leads to the decreased generation of NAD(P)H. These differences might cause the decreased expression of the second NADH dehydrogenase (Fig. 3). It was reported that strain AM1 cells contain more ATP when grown on methanol and more reducing equivalents [NAD(P)H] when grown on succinate (34). Thus, the higher expression of the ATPase complex under the methanol conditions (Fig. 3) was in accordance with the results from strain AM1, and the slight increase under the MLa condition suggested even higher ATP levels under this condition. These changes in the formaldehyde oxidation and respiratory chain could be a response to

the direct oxidation of methanol by XoxF1 and the concomitant decreased production of NAD(P)H.

Even when the concentration of methanol is limited, strain 22A showed comparable growth rates and cell yield in the presence and absence of La^{3+} (Fig. 1B). This result suggested that something other than methanol is the limiting factor for the growth rates. Since the direct oxidation of methanol to formate by XoxF1 allows less energy to be conserved [compared to the sequential oxidation of methanol by the MxaF and NAD(P)-dependent formaldehyde dehydrogenation pathways], one may expect a higher growth rate and lower cell yield in the presence of La^{3+}, but this was not the case under our experimental condition. The lower cell yield of the *mxaF* mutant compared to the wild type in the presence of La^{3+} (Fig. 1C) might suggest that *mxaF* also takes part in the methanol metabolism in the wild type, even in the presence of La^{3+}, or that lower energy conservation decreased the cell yield. Interestingly, this lowered cell yield does not occur in strain AM1 (10, 13). The MDH activity detected in strain 22A cells grown on methanol in the absence of La^{3+} (3 mU·mg^{-1} protein) was considerably lower than that in the presence of La^{3+} (49 mU·mg^{-1} protein) (Fig. 7A). These activities reflect the activity of MxaFI and XoxF1 (Fig. 4), but are contradictory to the comparative growth rates (Fig. 1C) of the wild type. The cell extract might contain unknown inhibitory factor(s) for MxaFI, or the enzyme might be unstable. It is also known that the range of MDH activities based on the phenazine methosulfate (PMS) and dichlorophenol indophenol (DCPIP) assay system is variable depending on the protocols (64 to 540 mU·mg^{-1} protein) (35). Thus, biochemical and enzymological characterization of MDHs in strain 22A is necessary, and cellular metabolic flux analysis is required to determine the carbon flow in the methanol metabolism in the presence of lanthanides.

In addition to MDH genes, other putative PQQ-containing dehydrogenase genes (c07235 and 1p30675) were also responsive to La^{3+} (Fig. 6). In strain AM1, ExaA (*META1_1139*) was revealed to be a lanthanide-dependent ethanol dehydrogenase that can oxidize ethanol and acetaldehyde, as well as methanol and formaldehyde, which conferred the growth of an *mxaF xoxF1 xoxF2* mutant on methanol (33). The protein is most homologous to c07235 in strain 22A (37% identity). The substrate specificity and biological function of the proteins encoded by these genes are currently unclear.

The presence of lanthanides induced expression of AT-rich genes in strain 22A, whose functions are unlikely to be important for methylotrophy (Fig. 5); this is intriguing as a biological response to lanthanides, however. Since AT-rich regions in bacterial genomes could be xenogeneic, controlling their expression is pivotal, as seen in *Pseudomonas aeruginosa* (36) and *Escherichia coli* (37). In *E. coli*, the abundance of NAPs depends on the growth phase, and the abundance of H-NS, HU, and Lrp sharply peaks in the exponential growth phase (38). Thus, we could not rule out that the small differences in the growth phase of the harvested cultures might affect the abundance of the transcripts of these genes. As their expression levels were not specifically low under lanthanide-containing conditions (Fig. S4), however, NAPs may not be involved in AT-rich gene induction. Another hypothesis is La^{3+}-induced DNA structural modification and the resultant enhanced transcription. Double-strand DNA forms two conformations: right-handed B-DNA (the natural form *in vivo*) and left-handed Z-DNA. Although Z-DNA formation requires extreme ionic strength (4 M NaCl), it is correlated with transcriptional activity. Recently, it was shown that lanthanide ions at millimolar levels were loaded to the grooves of DNA and stabilize the Z-DNA conformation with sequence sensitivity (39). It is unknown whether this is also the case for the observed phenomenon.

The strain 22A genome contains 28 genes for diguanylate cyclase or phosphodiesterase, among which 1p35125 showed the highest expression under the MLa condition (Fig. 6). This protein contains the GGDEF domain, regulating cell surface structures, including exopolysaccharide synthesis, biofilm formation, and motility (40). It is also encoded near *xoxF4-* and *xoxF5*-type genes in some methylotrophic bacteria (16), although this is not the case for strain 22A. Lanthanides induced exopolysaccharide

production in *Bradyrhizobium* sp. strain MAFF211645 (41). We did not recognize any difference in the colony morphology, motility, and biofilm formation (Fig. S6) in strain 22A. Thus, the function of the gene remains unclear at the moment.

The *rhs* (rearrangement hot spot) gene 1p37755 is located in a cluster containing two other *rhs* genes. These three *rhs* genes flank two AT-rich regions containing 1p37745, 1p37750, and 1p37760 with high expression in the presence of lanthanides (Fig. 5). Thus, the expression of *rhs* might be influenced by the upregulation of these AT-rich genes. Homologues of most, if not all, of these genes (*rhs* and AT-rich genes) are conserved even in different classes of bacteria. Furthermore, these *rhs* genes are linked to type VI secretion systems (T6SS), suggesting a possible mechanism of Rhs delivery (42, 43). A gene encoding the bacteriophage tail assembly protein involved in T6SS was also found to respond to La^{3+} (c04155, Fig. 6). Thus, there might be a link between lanthanides and T6SS induction, and it is tempting to hypothesize that lanthanides induce the competition machinery in *Methylobacterium*.

The amino acid sequence of c02050, annotated as "histidine kinase," contains a signal peptide and an EF-hand calcium-binding motif, but no kinase domain. EF-hand motifs are known to bind lanthanides (44, 45). The gene is conserved in many *Methylobacterium* and *Bradyrhizobium* genomes with high homology ($>55\%$ identity) and is also annotated as coding for a "calcium-binding protein." Its La^{3+}-dependent induction and possible metal binding imply that it binds lanthanides in the periplasm. The function of the gene is under investigation.

In conclusion, the presence of La^{3+} impacted the expression of both MDH genes and genes involved in the downstream pathway, possibly due to formaldehyde oxidation by XoxF1. In addition to methylotrophy genes, AT-rich genes and those possibly involved in cell survival were found to be upregulated in the presence of lanthanides. The validation of the importance of these genes through biochemical and genetic characterization will enhance our understanding of microbial methylotrophy in environments where lanthanides are present.

MATERIALS AND METHODS

Generation of MDH gene deletion mutants of *M. aquaticum* strain 22A. Strain 22A *mxaF* and *xoxF1* were subjected to deletion mutagenesis. Genomic regions containing each of these genes (ca. 4 kb) were PCR amplified using primers mxaf-UP (5'-TCGAGCTCGGTACCCGAGGTCTCGACCGGCATCGCC TCGGGGAA-3') and mxaf-DOWN (5'-CTCTAGAGGATCCCCTCGACTGGTCGAACCGCATCGCGACCTT-3') for *mxaF* and xoxf-UP (5'-TCGAGCTCGGTACCCACCCATGTCCACCCCGACCACGTGC-3') and xoxf-DOWN (5'-C TCTAGAGGATCCCCAGCTTCACCTTCAGCTCGTCGGCGA-3') for *xoxF1* and cloned into the SmaI site in pK18mobSacB (46) using the In-Fusion cloning kit (TaKaRa Bio Co.). Next, the regions of the ORFs were eliminated by inverse PCR with KOD DNA polymerase (Toyobo Co.) using primers Inv-mxaf-UP (5'-GTT CAGCGTCTCCAATCGGC-3') and Inv-mxaf-DOWN (5'-TCCGCCGATCCAGCGCTCCT-3') for *mxaF* and Inv-xoxf1-UP (5'-GGATTCCTCCGACAGGTGCA-3') and Inv-xoxf1-DOWN (5'-CGCGCGCCCGCACATCAGAC-3') for *xoxF1*, and the amplified fragments were circularized with polynucleotide kinase and T4 DNA ligase. The transformation of the plasmids into strain 22A, selection of double-crossover mutants, and diagnosis were carried out as described previously (47).

Cultivation conditions for RNA-seq. *M. aquaticum* strain 22A was grown in 100 ml mineral medium (MM; prepared without $CaCl_2$) (47) containing 0.5% (wt/vol) succinate and 30 μM $CaCl_2$ (called the SCa condition) or 0.5% (vol/vol) methanol (the methanol condition) with different metal supplementations in 500-ml glass culture flasks. As metal supplements, 30 μM each $CaCl_2$ (the MCa condition), $LaCl_3$ (MLa), $CaCl_2$ plus $LaCl_3$ (MCaLa), $CaCl_2$ plus $HoCl_3$ (MCaHo), and $CaCl_2$ plus $LuCl_3$ (MCaLu) was added. The flasks were washed with 1 M HCl prior to use. For the MLa condition, we did not add $CaCl_2$, but the medium was not free from Ca^{2+} since it is impossible to eliminate calcium ions completely; therefore, the cells grew normally even under the MLa condition. The flasks were shaken at 200 rpm at 28°C for 38 to 84 h. In the log phase of growth (optical density at 600 nm [OD_{600}] of 0.3 to 0.4), the cells were harvested by centrifugation at 6,500 $\times$ *g* at 4°C for 5 min and frozen with liquid nitrogen. The cultivation was carried out in triplicate.

For growth experiments, strain 22A and its MDH gene deletion mutants were grown in 200 μl MM containing 30 μM $CaCl_2$ prepared in 96-well plates at 28°C with rotary shaking at 300 rpm. Growth (OD_{600}) was measured using a microplate reader (PowerScan HT, DS Pharma Biomedical) without dilution and a factor of 3.42 to convert the readings to a 1-cm light path. The readings of the microplate reader were linear up to an OD_{600} of 1.0 (3.42 with a 1-cm light path).

RNA-seq. The frozen cells were subjected to total RNA extraction by the hot phenol extraction method (48). DNA was digested with RQ1 RNase-free DNase I (Promega, Fitchburg, WI). Next, rRNA was depleted using Ribo-Zero rRNA removal kits (Gram-negative bacteria) (Epicentre) according to the

manufacturer's protocol. The rRNA-depleted samples were subjected to single-read sequencing on an Illumina HiSeq 2500 system.

Mapping and data analysis. The reads were mapped to the sequences of six replicons of the strain 22A genome and the coding DNA sequence (CDS) list containing rRNA sequences using BWA (49) at Maser (https://cell-innovation.nig.ac.jp). The reads mapped to ribosomal RNAs were subtracted from the total mapped reads to count reads mapped to CDSs and to calculate reads per kilobase per million (RPKM) based on read counts to CDSs (but not total reads). Since samples of MLa and MCaLu were sequenced on a 100-base platform, the read data were trimmed to 36 bases for mapping. Differential abundance analysis was done with DESeq2 1.18.0 (50) of the R package (version 3.3.3) (51).

MDH activity assay. Strain 22A was cultured on 0.5% (vol/vol) methanol or 0.5 (wt/vol) succinate in 1 liter MM in the absence or presence of 30 μM LaCl$_3$ at 28°C for 3 days. The cells were collected, suspended in 50 mM morpholineethanesulfonic acid (MES)–NaOH buffer (pH 5.5), and disrupted with a Mini-BeadBeater (BioSpec 3110BX; Ieda Trading Corporation). The samples were centrifuged at 10,000 × g at 4°C for 10 min. The supernatant was used as cell extract and subjected to the MDH activity assay. The reaction mixture in 96-well plates contained 158 μl of 100 mM Tris-HCl (pH 9.0), 2 μl of 1.5 M ammonium chloride, 10 μl of 6.6 mM phenazine methosulfate (PMS), 10 μl of 1 mM dichlorophenol indophenol (DCPIP), and 10 μl of enzyme solution. After incubation at 30°C for 5 to 10 min when the dye bleaching stabilized, 10 μl of 20 mM methanol was added to initiate the reaction. The change at 600 nm was monitored using a microplate reader (PowerScan HT). Protein concentrations were measured by the Bradford method with bovine serum albumin as the standard. The specific activity was calculated based on a molar extinction coefficient at 600 nm for DCPIP of 19,000 M^{-1}·cm^{-1} and a factor of 1.62 to convert the microplate readings to a 1-cm light path. One unit of activity was defined as the enzyme amount that catalyzes the oxidation of 1 μmol of the substrate. Instead of methanol, the same concentration of formaldehyde (prepared by autoclaving paraformaldehyde solution) was also tested as a substrate.

Formaldehyde production and degradation in resting cell reaction. Strain 22A cells, grown on solid MM containing 0.5% methanol in the presence and absence of 30 μM LaCl$_3$ at 28°C for 2 days, were washed with HEPES buffer (10 mM, pH 7.0). The cell density was adjusted to an OD$_{600}$ of 0.1 (formaldehyde production) or 0.5 (formaldehyde degradation) in HEPES buffer, and the cells grown in the presence of LaCl$_3$ were suspended in the buffer containing 30 μM LaCl$_3$. The cell suspensions were aliquoted to 96-well plates (180 μl). For formaldehyde production, 20 μl of 20% methanol was added, and the plates were incubated at 28°C for 90 min. At the appropriate time, 20 μl of trichloroacetic acid was added to terminate the reaction. The plates were centrifuged at 2,000 × g for 5 min, and 100 μl of the supernatant was transferred into new plates containing 100 μl of 15% (wt/vol) ammonium acetate, 0.3% (vol/vol) acetic acid, and 0.2% (vol/vol) acetylacetone (52). The plates were incubated at 30°C for 30 min, and absorbance at 410 nm was measured using a microplate reader (PowerScan HT). A solution of formaldehyde (0 to 1 mM) served as the standard. For formaldehyde degradation, 20 μl of 5 mM formaldehyde was added to the wells, and the subsequent procedure was performed the same as described above. The cell suspensions were spread onto R2A plate medium for CFU determination. As controls, autoclave-killed cell suspensions (120°C for 15 min) were used. The data were analyzed by Sidak's multiple-comparison test using Prism 6.0f (GraphPad Software, Inc.).

Analytical methods. PQQ content in the spent culture supernatant of strain 22A grown under different conditions was measured by high-performance liquid chromatography (HPLC) on a chromatograph equipped with a fluorescence detector as reported previously (53). For biofilm quantification, strain 22A was grown on 0.5% (vol/vol) methanol or 0.5% (wt/vol) succinate in the absence or presence of 30 μM LaCl$_3$ in 200 μl MM prepared in 96-well plates at 28°C for 1 week. On days 3 and 7 after inoculation, the media were removed and the wells were washed with water three times. Next, the plates were dried for 45 min at room temperature, and 200 μl of 0.5% crystal violet was added. After 45 min of incubation at room temperature, the wells were washed five times, and 200 μl of 95% ethanol was added. The absorbance of the samples at 595 nm was measured, and A_{595} (OD$_{600}$ of the culture) was used for evaluation of biofilm formation. Statistical analysis was done with Prism 6.0h (GraphPad Software, Inc.).

Data availability. The RNA-seq raw data have been deposited into DDBJ under GenBank accession no. DRA002908.

SUPPLEMENTAL MATERIAL

Supplemental material for this article may be found at https://doi.org/10.1128/mSphere.00462-17.

FIG S1, TIF file, 0.1 MB.
FIG S2, TIF file, 0.2 MB.
FIG S3, TIF file, 0.2 MB.
FIG S4, TIF file, 0.1 MB.
FIG S5, TIF file, 0.1 MB.
FIG S6, TIF file, 0.1 MB.
TABLE S1, XLSX file, 0.1 MB.
TABLE S2, XLSX file, 0.1 MB.
TABLE S3, TXT file, 2.2 MB.

REFERENCES

1. Green PN. 2006. Methylobacterium, p 257–265. In Dworkin M, Falkow S, Rosenberg E, Schleifer K-H, Stackebrandt E (ed), The prokaryotes. Springer, New York, NY.
2. Delmotte N, Knief C, Chaffron S, Innerebner G, Roschitzki B, Schlapbach R, von Mering C, Vorholt JA. 2009. Community proteogenomics reveals insights into the physiology of phyllosphere bacteria. Proc Natl Acad Sci U S A 106:16428–16433. https://doi.org/10.1073/pnas.0905240106.
3. Anthony C. 2011. How half a century of research was required to understand bacterial growth on C1 and C2 compounds; the story of the serine cycle and the ethylmalonyl-CoA pathway. Sci Prog 94:109–137. https://doi.org/10.3184/003685011X13044430633960.
4. Chistoserdova L. 2011. Modularity of methylotrophy, revisited. Environ Microbiol 13:2603–2622. https://doi.org/10.1111/j.1462-2920.2011.02464.x.
5. Anthony C. 2000. Methanol dehydrogenase, a PQQ-containing quinoprotein dehydrogenase, p 73–117. In Holzenburg A, Scrutton NS (ed), Enzyme-catalyzed electron and radical transfer. Springer, Boston, MA.
6. Skovran E, Palmer AD, Rountree AM, Good NM, Lidstrom ME. 2011. XoxF is required for expression of methanol dehydrogenase in Methylobacterium extorquens AM1. J Bacteriol 193:6032–6038. https://doi.org/10.1128/JB.05367-11.
7. Schmidt S, Christen P, Kiefer P, Vorholt JA. 2010. Functional investigation of methanol dehydrogenase-like protein XoxF in Methylobacterium extorquens AM1. Microbiology 156:2575–2586. https://doi.org/10.1099/mic.0.038570-0.
8. Hibi Y, Asai K, Arafuka H, Hamajima M, Iwama T, Kawai K. 2011. Molecular structure of La^{3+}-induced methanol dehydrogenase-like protein in Methylobacterium radiotolerans. J Biosci Bioeng 111:547–549. https://doi.org/10.1016/j.jbiosc.2010.12.017.
9. Fitriyanto NA, Fushimi M, Matsunaga M, Pertiwiningrum A, Iwama T, Kawai K. 2011. Molecular structure and gene analysis of Ce^{3+}-induced methanol dehydrogenase of Bradyrhizobium sp. MAFF211645. J Biosci Bioeng 111:613–617. https://doi.org/10.1016/j.jbiosc.2011.01.015.
10. Nakagawa T, Mitsui R, Tani A, Sasa K, Tashiro S, Iwama T, Hayakawa T, Kawai K. 2012. A catalytic role of XoxF1 as La^{3+}-dependent methanol dehydrogenase in Methylobacterium extorquens strain AM1. PLoS One 7:e50480. https://doi.org/10.1371/journal.pone.0050480.
11. Pol A, Barends TRM, Dietl A, Khadem AF, Eygensteyn J, Jetten MSM, Op den Camp HJM. 2014. Rare earth metals are essential for methanotrophic life in volcanic mudpots. Environ Microbiol 16:255–264. https://doi.org/10.1111/1462-2920.12249.
12. Chistoserdova L. 2016. Lanthanides: new life metals? World J Microbiol Biotechnol 32:138. https://doi.org/10.1007/s11274-016-2088-2.
13. Vu HN, Subuyuj GA, Vijayakumar S, Good NM, Martinez-Gomez NC, Skovran E. 2016. Lanthanide-dependent regulation of methanol oxidation systems in Methylobacterium extorquens AM1 and their contribution to methanol growth. J Bacteriol 198:1250–1259. https://doi.org/10.1128/JB.00937-15.
14. Chu F, Lidstrom ME. 2016. XoxF acts as the predominant methanol dehydrogenase in the type I methanotroph Methylomicrobium buryatense. J Bacteriol 198:1317–1325. https://doi.org/10.1128/JB.00959-15.
15. Chu F, Beck DAC, Lidstrom ME. 2016. MxaY regulates the lanthanide-mediated methanol dehydrogenase switch in Methylomicrobium buryatense. PeerJ 4:e2435. https://doi.org/10.7717/peerj.2435.
16. Keltjens JT, Pol A, Reimann J, Op den Camp HJM. 2014. PQQ-dependent methanol dehydrogenases: rare-earth elements make a difference. Appl Microbiol Biotechnol 98:6163–6183. https://doi.org/10.1007/s00253-014-5766-8.
17. Moermond CTA, Tijink J, van Wezel AP, Koelmans AA. 2001. Distribution, speciation, and bioavailability of lanthanides in the Rhine-Meuse estuary, The Netherlands. Environ Toxicol Chem 20:1916–1926. https://doi.org/10.1002/etc.5620200909.
18. Tyler G, Olsson T. 2005. Rare earth elements in forest-floor herbs as related to soil conditions and mineral nutrition. Biol Trace Elem Res 106:177–191. https://doi.org/10.1385/BTER:106:2:177.
19. Tyler G. 2004. Rare earth elements in soil and plant systems—a review. Plant Soil 267:191–206. https://doi.org/10.1007/s11104-005-4888-2.
20. Tani A, Takai Y, Suzukawa I, Akita M, Murase H, Kimbara K. 2012. Practical application of methanol-mediated mutualistic symbiosis between Methylobacterium species and a roof greening moss, Racomitrium japonicum. PLoS One 7:e33800. https://doi.org/10.1371/journal.pone.0033800.
21. Tani A, Ogura Y, Hayashi T, Kimbara K. 2015. Complete genome sequence of Methylobacterium aquaticum strain 22A, isolated from Racomitrium japonicum moss. Genome Announc 3:e00266-15. https://doi.org/10.1128/genomeA.00266-15.
22. Tani A, Sahin N, Fujitani Y, Kato A, Sato K, Kimbara K. 2015. Methylobacterium species promoting rice and barley growth and interaction specificity revealed with whole-cell matrix-assisted laser desorption/ionization-time-of-flight mass spectrometry (MALDI-TOF/MS) analysis. PLoS One 10:e0129509. https://doi.org/10.1371/journal.pone.0129509.
23. Springer AL, Morris CJ, Lidstrom ME. 1997. Molecular analysis of mxbD and mxbM, a putative sensor-regulator pair required for oxidation of methanol in Methylobacterium extorquens AM1. Microbiology 143:1737–1744. https://doi.org/10.1099/00221287-143-5-1737.
24. Springer AL, Chou HH, Fan WH, Lee E, Lidstrom ME. 1995. Methanol oxidation mutants in Methylobacterium extorquens AM1: identification of new genetic complementation groups. Microbiology 141:2985–2993. https://doi.org/10.1099/13500872-141-11-2985.
25. Goenrich M, Bartoschek S, Hagemeier CH, Griesinger C, Vorholt JA. 2002. A glutathione-dependent formaldehyde-activating enzyme (Gfa) from Paracoccus denitrificans detected and purified via two-dimensional proton exchange NMR spectroscopy. J Biol Chem 277:3069–3072. https://doi.org/10.1074/jbc.C100579200.
26. Hemmann JL, Saurel O, Ochsner AM, Stodden BK, Kiefer P, Milon A, Vorholt JA. 2016. The one-carbon carrier methylofuran from Methylobacterium extorquens AM1 contains a large number of α- and γ-linked glutamic acid residues. J Biol Chem 291:9042–9051. https://doi.org/10.1074/jbc.M116.714741.
27. Erb TJ, Berg IA, Brecht V, Müller M, Fuchs G, Alber BE. 2007. Synthesis of C5-dicarboxylic acids from C2-units involving crotonyl-CoA carboxylase/reductase: the ethylmalonyl-CoA pathway. Proc Natl Acad Sci U S A 104:10631–10636. https://doi.org/10.1073/pnas.0702791104.
28. Peyraud R, Kiefer P, Christen P, Massou S, Portais JC, Vorholt JA. 2009. Demonstration of the ethylmalonyl-CoA pathway by using ^{13}C metabolomics. Proc Natl Acad Sci U S A 106:4846–4851. https://doi.org/10.1073/pnas.0810932106.
29. Howitt CA, Udall PK, Vermaas WF. 1999. Type 2 NADH dehydrogenases in the cyanobacterium Synechocystis sp. strain PCC 6803 are involved in regulation rather than respiration. J Bacteriol 181:3994–4003.
30. Heikal A, Nakatani Y, Dunn E, Weimar MR, Day CL, Baker EN, Lott JS, Sazanov LA, Cook GM. 2014. Structure of the bacterial type II NADH dehydrogenase: a monotopic membrane protein with an essential role in energy generation. Mol Microbiol 91:950–964. https://doi.org/10.1111/mmi.12507.
31. Singh SS, Singh N, Bonocora RP, Fitzgerald DM, Wade JT, Grainger DC. 2014. Widespread suppression of intragenic transcription initiation by H-NS. Genes Dev 28:214–219. https://doi.org/10.1101/gad.234336.113.
32. Shintani M, Suzuki-Minakuchi C, Nojiri H. 2015. Nucleoid-associated proteins encoded on plasmids: occurrence and mode of function. Plasmid 80:32–44. https://doi.org/10.1016/j.plasmid.2015.04.008.
33. Good NM, Vu HN, Suriano CJ, Subuyuj GA, Skovran E, Martinez-Gomez NC. 2016. Pyrroloquinoline quinone-containing ethanol dehydrogenase in Methylobacterium extorquens AM1 extends lanthanide-dependent metabolism to multicarbon substrates. J Bacteriol 198:3109–3118. https://doi.org/10.1128/JB.00478-16.
34. Guo X, Lidstrom ME. 2006. Physiological analysis of Methylobacterium

extorquens AM1 grown in continuous and batch cultures. Arch Microbiol 186:139–149. https://doi.org/10.1007/s00203-006-0131-7.

35. Šmejkalová H, Erb TJ, Fuchs G. 2010. Methanol assimilation in *Methylobacterium extorquens* AM1: demonstration of all enzymes and their regulation. PLoS One 5:e13001. https://doi.org/10.1371/journal.pone.0013001.

36. Castang S, Dove SL. 2012. Basis for the essentiality of H-NS family members in *Pseudomonas aeruginosa*. J Bacteriol 194:5101–5109. https://doi.org/10.1128/JB.00932-12.

37. Müller CM, Dobrindt U, Nagy G, Emödy L, Uhlin BE, Hacker J. 2006. Role of histone-like proteins H-NS and StpA in expression of virulence determinants of uropathogenic *Escherichia coli*. J Bacteriol 188:5428–5438. https://doi.org/10.1128/JB.01956-05.

38. Ali Azam T, Iwata A, Nishimura A, Ueda S, Ishihama A. 1999. Growth phase-dependent variation in protein composition of the *Escherichia coli* nucleoid. J Bacteriol 181:6361–6370.

39. Nayak AK, Mishra A, Jena BS, Mishra BK, Subudhi U. 2016. Lanthanum induced B-to-Z transition in self-assembled Y-shaped branched DNA structure. Sci Rep 6:26855. https://doi.org/10.1038/srep26855.

40. Schirmer T, Jenal U. 2009. Structural and mechanistic determinants of c-di-GMP signalling. Nat Rev Microbiol 7:724–735. https://doi.org/10.1038/nrmicro2203.

41. Fitriyanto NA, Nakamura M, Muto S, Kato K, Yabe T, Iwama T, Kawai K, Pertiwiningrum A. 2011. Ce^{3+}-induced exopolysaccharide production by *Bradyrhizobium* sp. MAFF211645. J Biosci Bioeng 111:146–152. https://doi.org/10.1016/j.jbiosc.2010.09.008.

42. Koskiniemi S, Lamoureux JG, Nikolakakis KC, t'Kint de Roodenbeke C, Kaplan MD, Low DA, Hayes CS. 2013. Rhs proteins from diverse bacteria mediate intercellular competition. Proc Natl Acad Sci U S A 110:7032–7037. https://doi.org/10.1073/pnas.1300627110.

43. Silverman JM, Brunet YR, Cascales E, Mougous JD. 2012. Structure and regulation of the type VI secretion system. Annu Rev Microbiol 66:453–472. https://doi.org/10.1146/annurev-micro-121809-151619.

44. Ma C, Opella SJ. 2000. Lanthanide ions bind specifically to an added "EF-hand" and orient a membrane protein in micelles for solution NMR spectroscopy. J Magn Reson 146:381–384. https://doi.org/10.1006/jmre.2000.2172.

45. Lim S, Franklin SJ. 2004. Lanthanide-binding peptides and the enzymes that might have been. Cell Mol Life Sci 61:2184–2188. https://doi.org/10.1007/s00018-004-4156-2.

46. Schäfer A, Tauch A, Jäger W, Kalinowski J, Thierbach G, Pühler A. 1994. Small mobilizable multi-purpose cloning vectors derived from the Escherichia coli plasmids pK18 and pK19: selection of defined deletions in the chromosome of Corynebacterium glutamicum. Gene 145:69–73. https://doi.org/10.1016/0378-1119(94)90324-7.

47. Alamgir KM, Masuda S, Fujitani Y, Fukuda F, Tani A. 2015. Production of ergothioneine by *Methylobacterium* species. Front Microbiol 6:1185. https://doi.org/10.3389/fmicb.2015.01185.

48. Babst M, Hennecke H, Fischer HM. 1996. Two different mechanisms are involved in the heat-shock regulation of chaperonin gene expression in *Bradyrhizobium japonicum*. Mol Microbiol 19:827–839. https://doi.org/10.1046/j.1365-2958.1996.438968.x.

49. Li H, Durbin R. 2009. Fast and accurate short read alignment with Burrows-Wheeler transform. Bioinformatics 25:1754–1760. https://doi.org/10.1093/bioinformatics/btp324.

50. Love MI, Huber W, Anders S. 2014. Moderated estimation of fold change and dispersion for RNA-seq data with DESeq2. Genome Biol 15:550. https://doi.org/10.1186/s13059-014-0550-8.

51. R Development Core Team. 2011. R: a language and environment for statistical computing. R Foundation for Statistical Computing, Vienna, Austria.

52. Nash T. 1953. The colorimetric estimation of formaldehyde by means of the Hantzsch reaction. Biochem J 55:416–421. https://doi.org/10.1042/bj0550416.

53. Tani A, Sahin N, Matsuyama Y, Enomoto T, Nishimura N, Yokota A, Kimbara K. 2012. High-throughput identification and screening of novel *Methylobacterium* species using whole-cell MALDI-TOF/MS analysis. PLoS One 7:e40784. https://doi.org/10.1371/journal.pone.0040784.